ARTICLE

doi:10.1038/nature11732

Non-Fermi-liquid *d*-wave metal phase of strongly interacting electrons

Hong-Chen Jiang[1], Matthew S. Block[2], Ryan V. Mishmash[3], James R. Garrison[3], D. N. Sheng[4], Olexei I. Motrunich[5] & Matthew P. A. Fisher[3]

Developing a theoretical framework for conducting electronic fluids qualitatively distinct from those described by Landau's Fermi-liquid theory is of central importance to many outstanding problems in condensed matter physics. One such problem is that, above the transition temperature and near optimal doping, high-transition-temperature copper-oxide superconductors exhibit 'strange metal' behaviour that is inconsistent with being a traditional Landau Fermi liquid. Indeed, a microscopic theory of a strange-metal quantum phase could shed new light on the interesting low-temperature behaviour in the pseudogap regime and on the *d*-wave superconductor itself. Here we present a theory for a specific example of a strange metal—the '*d*-wave metal'. Using variational wavefunctions, gauge theoretic arguments, and ultimately large-scale density matrix renormalization group calculations, we show that this remarkable quantum phase is the ground state of a reasonable microscopic Hamiltonian—the usual *t*–*J* model with electron kinetic energy *t* and two-spin exchange *J* supplemented with a frustrated electron 'ring-exchange' term, which we here examine extensively on the square lattice two-leg ladder. These findings constitute an explicit theoretical example of a genuine non-Fermi-liquid metal existing as the ground state of a realistic model.

Over the past several decades, experiments on strongly correlated materials have routinely revealed, in certain parts of the phase diagram, conducting liquids with physical properties that are qualitatively inconsistent with Landau's Fermi-liquid theory[1]. Examples of these 'non-Fermi-liquid' metals[2] include the strange-metal phase of the copper-oxide superconductors[3,4] and the heavy fermion materials near a quantum critical point[5,6]. However, such non-Fermi-liquid behaviour has been challenging to characterize theoretically, largely owing to the lack of a weakly interacting quasiparticle description. It is even difficult to define a non-Fermi liquid unambiguously, although possible deviations from Fermi-liquid theory include, for example, violation of Luttinger's volume theorem[7], vanishing quasiparticle weight, and anomalous thermodynamics and transport[5,8–12]. This theoretical difficulty is probably preventing a full understanding of the mechanism behind high-temperature superconductivity and also hampering theoretically guided searches for new exotic materials.

Pioneering early theoretical work on the copper oxides relied on two main premises[3,13–17], which guide but do not constrain our pursuit of non-Fermi-liquid physics: (1) that the microscopic behaviour can be described by the square lattice Hubbard model with on-site Coulomb repulsion, which at strong coupling reduces in its simplest form to the *t*–*J* model; and (2) that the physics of the system can be faithfully represented by the 'slave-boson' technique, in which the physical electron operator is written as the product of a slave boson ('chargon'), which carries the electronic charge, and a spin-half fermionic 'spinon'[18], which carries the spin (both chargon and spinon are strongly coupled to an emergent gauge field). However, within the slave-boson formulation, it has been difficult to access non-Fermi-liquid physics at low temperatures because this requires the chargons to be in an uncondensed, yet conducting, quantum phase[19]—the elusive 'Bose metal'. Early attempts to describe the strange metal in this framework treated it as a strictly finite-temperature phenomenon in which the slave bosons form an uncondensed, but classical, Bose fluid[15,16], a treatment which excludes the possibility that the strange metal is a true quantum phase at all.

In our view, the strange metal should be viewed as a genuine two-dimensional (2D) quantum phase, which may be unstable to superconducting or pseudogap behaviour. Indeed, recent experimental work on $La_{2-x}Sr_xCuO_4$ has shown that when superconductivity is stripped away by high magnetic fields, strange-metal behaviour persists over a wide doping range down to extremely low temperatures[20]. Thus, the strange metal in the copper oxides is quite possibly a true, extended, zero-temperature quantum phase[4].

Inspired by these results and building on our previous work, which proposed[21] and realized[22–24] a true, zero-temperature Bose metal, we use a variant of the slave-boson approach to construct and analyse an exotic 2D non-Fermi-liquid quantum phase, which we refer to as the '*d*-wave metal'. The *d*-wave metal is modelled by a variational wavefunction consisting of a product of a *d*-wave Bose-metal wavefunction[21–24] for the chargons and a usual Slater determinant for the spinons. Importantly, placing the chargons in the *d*-wave Bose metal state provides the many-electron wavefunction with a sign structure that is qualitatively distinct from that of a simple Slater determinant, and in particular, imprints strong singlet *d*-wave two-particle correlations. This results in a gapless, conducting quantum fluid with an electron momentum distribution function that exhibits a critical, singular surface that violates Luttinger's volume theorem[7], as well as prominent critical Cooper pairs with *d*-wave character. The *d*-wave nature of our phase is tantalizingly suggestive of incipient *d*-wave superconductivity and is thus of possible relevance to the copper oxides.

Furthermore, tying back into premise (1) above, we propose a reasonably simple model Hamiltonian to stabilize the *d*-wave metal by augmenting the traditional *t*–*J* model with a four-site ring-exchange

[1]Kavli Institute for Theoretical Physics, University of California, Santa Barbara, California 93106, USA. [2]Department of Physics and Astronomy, University of Kentucky, Lexington, Kentucky 40506, USA. [3]Department of Physics, University of California, Santa Barbara, California 93106, USA. [4]Department of Physics and Astronomy, California State University, Northridge, California 91330, USA. [5]Department of Physics, California Institute of Technology, Pasadena, California 91125, USA.

term K. Then, thanks to the numerical and analytical tractability provided by the density matrix renormalization group (DMRG)[25,26] and bosonization[27–30], we can place the problem on a quasi-one-dimensional (1D) two-leg ladder geometry (see Fig. 1). In this system, we establish several lines of compelling evidence that the d-wave metal phase exists as the quantum ground state of our t–J–K model Hamiltonian, and we are able to characterize and understand the phase very thoroughly. Importantly, our realized two-leg d-wave metal state is non-perturbative, in that it cannot be understood within conventional Luttinger liquid theory[27] starting from free electrons[31]. We believe this study to be one of the first unbiased numerical demonstrations of a non-Fermi-liquid metal as the stable ground state of a local Hamiltonian. We also discuss straightforward extensions of these results to two dimensions, and comment on their potential relevance to the actual non-Fermi liquids observed in experiments.

Gauge theory and variational wavefunctions

Our theoretical description of the non-Fermi-liquid d-wave metal begins by writing the electron operator for site $\boldsymbol{r}$ and spin state $s = \uparrow, \downarrow$ as the product of a bosonic chargon $b(\boldsymbol{r})$ and fermionic spinon $f_s(\boldsymbol{r})$; that is, $c_s(\boldsymbol{r}) = b(\boldsymbol{r})f_s(\boldsymbol{r})$. With $b(\boldsymbol{r})$ a hard-core boson operator, this construction prohibits doubly occupied sites, an assumption we make from here on. The physical electron Hilbert space is recovered by implementing at each site the constraint $b^\dagger(\boldsymbol{r})b(\boldsymbol{r}) = \sum_s f_s^\dagger(\boldsymbol{r})f_s(\boldsymbol{r}) = \sum_s c_s^\dagger(\boldsymbol{r})c_s(\boldsymbol{r}) = n_e(\boldsymbol{r})$, which physically means that a given site is either empty or contains a chargon and exactly one spinon to compose an electron. Theoretically, this is achieved by strongly coupling the b and f fields via an emergent gauge field[3].

Under the natural assumption that the spinons are in a Fermi-sea state, the behaviour of the chargons determines the resulting electronic phase. Condensing the bosonic chargons so that $\langle b(\boldsymbol{r})\rangle \neq 0$ implies $c_s(\boldsymbol{r}) \propto f_s(\boldsymbol{r})$; so, in this case, the electronic phase is that of a Fermi liquid. It then follows that to describe a non-Fermi-liquid conducting quantum fluid within this framework, the chargons must not condense, $\langle b(\boldsymbol{r})\rangle = 0$, but must still conduct. However, accessing such a 'Bose metal' phase has proved extremely difficult. In recent work[21–24], however, we have realized a concrete, genuine Bose-metal phase, which we named the "d-wave Bose liquid" or, equivalently, the "d-wave Bose metal" (DBM). The DBM is central to our construction of the d-wave metal. Specifically, in the DBM, we decompose the hard-core boson as $b(\boldsymbol{r}) = d_1(\boldsymbol{r})d_2(\boldsymbol{r})$ with the constraint $d_1^\dagger(\boldsymbol{r})d_1(\boldsymbol{r}) = d_2^\dagger(\boldsymbol{r})d_2(\boldsymbol{r}) = b^\dagger(\boldsymbol{r})b(\boldsymbol{r})$, where d_1 and d_2 are fermionic slave particles ('partons') with anisotropic hopping patterns: d_1 (d_2) is chosen to hop preferentially in the $\hat{x}$ ($\hat{y}$) direction. The resulting bosonic phase is a conducting, yet uncondensed, quantum fluid, which is precisely the phase into which we place the charge sector of the d-wave metal. That is, for the d-wave metal we take an all-fermionic decomposition of the electron

$$c_s(\boldsymbol{r}) = d_1(\boldsymbol{r})d_2(\boldsymbol{r})f_s(\boldsymbol{r}) \tag{1}$$

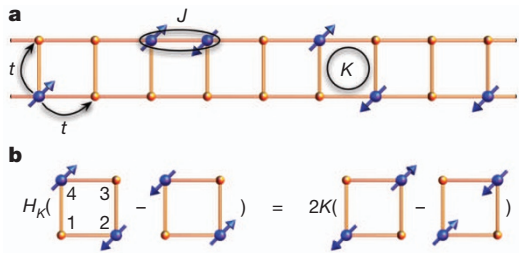

Figure 1 | Schematic of the t–J–K model Hamiltonian. **a**, Picture of the full t–J–K model, equation (6), on the two-leg ladder. We use periodic boundary conditions in the long ($\hat{x}$) direction for all calculations. **b**, Action of the ring term H_K, equation (8), on a single plaquette, elucidating its 'singlet-rotation' nature.

subject to the constraint

$$d_1^\dagger(\boldsymbol{r})d_1(\boldsymbol{r}) = d_2^\dagger(\boldsymbol{r})d_2(\boldsymbol{r}) = \sum_s f_s^\dagger(\boldsymbol{r})f_s(\boldsymbol{r}) = n_e(\boldsymbol{r}) \tag{2}$$

The resulting theory now includes two gauge fields: one to glue together d_1 and d_2 to form the chargon and another to glue together b and f to form the electron. In the Supplementary Information, we give a detailed bosonization analysis of this gauge theory for the two-leg ladder study (see below).

Guided by the slave-boson construction, one can naturally construct electronic variational wavefunctions by taking the product of a hard-core bosonic wavefunction ψ_b and a fermionic wave function ψ_f and evaluating them at the same coordinates (Gutzwiller projection):

$$\psi_c\left(\left\{\boldsymbol{r}_i^\uparrow\right\},\left\{\boldsymbol{r}_i^\downarrow\right\}\right) = \mathcal{P}_G\left[\psi_b(\{\boldsymbol{R}_i\}) \times \psi_f\left(\left\{\boldsymbol{r}_i^\uparrow\right\},\left\{\boldsymbol{r}_i^\downarrow\right\}\right)\right] \tag{3}$$

where $\mathcal{P}_G$ performs the projection into the physical electronic Hilbert space: $\{\boldsymbol{R}_i\} = \left\{\boldsymbol{r}_i^\uparrow\right\} \bigcup \left\{\boldsymbol{r}_i^\downarrow\right\}$. If we put the f partons into a spin-singlet Fermi-sea state with orbitals $\{\boldsymbol{k}_j\}$ (Slater determinant), that is, $\psi_f\left(\left\{\boldsymbol{r}_i^\uparrow\right\},\left\{\boldsymbol{r}_i^\downarrow\right\}\right) = \det\left[e^{i\boldsymbol{k}_j \cdot \boldsymbol{r}_i^\uparrow}\right] \det\left[e^{i\boldsymbol{k}_j \cdot \boldsymbol{r}_i^\downarrow}\right] = \psi_f^{FS}$, then we can model both the Fermi-liquid metal and the non-Fermi-liquid d-wave metal in a unified way. In both cases, the wavefunctions are straightforward to implement using variational Monte Carlo (VMC) methods[32–34].

For the Fermi liquid, we put the b partons into a superfluid wavefunction ψ_b^{SF} via a typical Jastrow form, so that, schematically, $\psi_c^{FL} = \mathcal{P}_G\left[\psi_b^{SF} \times \psi_f^{FS}\right]$. Given that ψ_b^{SF} is a positive wavefunction, the sign structure[35] of ψ_c^{FL} is identical to that of the non-interacting Fermi-sea state. In contrast, to model the d-wave metal, we put the b partons into a Bose-metal wavefunction according to the DBM construction of refs 21–24:

$$\psi_b(\{\boldsymbol{R}_i\}) = \psi_{d_1}(\{\boldsymbol{R}_i\}) \times \psi_{d_2}(\{\boldsymbol{R}_i\}) = \psi_b^{DBM} \tag{4}$$

where $\psi_{d_1}\left(\psi_{d_2}\right)$ is a Slater determinant with a Fermi sea compressed in the $\hat{x}$ ($\hat{y}$) direction[21]. Then, we have

$$\psi_c^{d\text{-wave metal}} = \mathcal{P}_G\left[\psi_b^{DBM} \times \psi_f^{FS}\right] = \mathcal{P}_G\left[\psi_{d_1} \times \psi_{d_2} \times \psi_f^{FS}\right] \tag{5}$$

Interestingly, this construction, equation (5), is actually a time-reversal invariant analogue of the composite Fermi-liquid description of the half-filled Landau level[36], where the d-wave Bose-metal wavefunction[21] has the role of Laughlin's $\nu = 1/2$ bosonic state[37]. Just as Laughlin's wavefunction imprints a nontrivial complex phase pattern on the Slater determinant, the DBM wavefunction imprints a non-trivial d-wave sign structure. There are many physical signatures associated with putting the chargons into the DBM phase, making the d-wave metal dramatically distinguishable from the traditional Landau Fermi liquid (see below).

Microscopic ring-exchange model

The t–J–K model Hamiltonian which we propose to stabilize the d-wave metal phase is given by

$$H = H_{tJ} + H_K \tag{6}$$

$$H_{tJ} = -t \sum_{\langle i,j\rangle, s=\uparrow,\downarrow} \left(c_{is}^\dagger c_{js} + c_{js}^\dagger c_{is}\right) + J \sum_{\langle i,j\rangle} \boldsymbol{S}_i \cdot \boldsymbol{S}_j \tag{7}$$

$$H_K = 2K \sum_{\square} \left(\mathcal{S}_{13}^\dagger \mathcal{S}_{24} + \mathcal{S}_{24}^\dagger \mathcal{S}_{13}\right) \tag{8}$$

where $\langle i,j\rangle$ and $\square$ indicate sums over all nearest-neighbour bonds and all elementary plaquettes of the 2D square lattice, respectively. In the

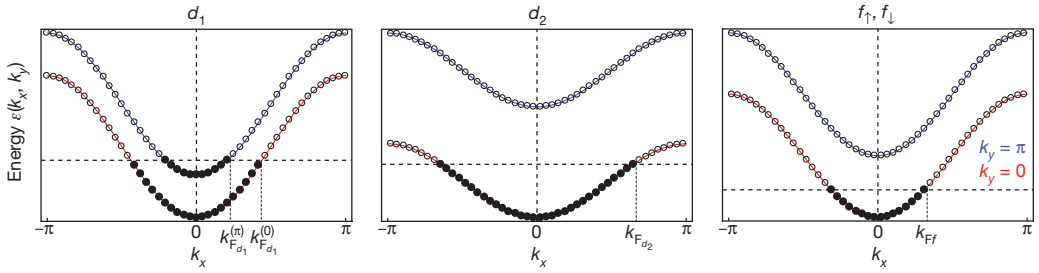

Figure 2 | Picture of the parton bands for the *d*-wave metal phase. We show orbitals for a 48×2 system, showing partially occupied bonding ($k_y = 0$) and antibonding ($k_y = \pi$) bands for d_1 and partially occupied bonding bands for d_2 and $f_{\uparrow/\downarrow}$; that is, each Slater determinant in equation (5) consists of momentum-space orbitals as depicted here. The total electron number is $N_e = N_{c\uparrow} + N_{c\downarrow} = N_{d_1} = N_{d_2} = N_{f\uparrow} + N_{f\downarrow} = 32$, with $N_{f\uparrow} = N_{f\downarrow} = 16$ so that $S_{tot} = 0$; the longitudinal boundary conditions are periodic for d_1 and antiperiodic for d_2 and $f_{\uparrow/\downarrow}$. This is precisely the same *d*-wave metal configuration for which we display characteristic measurements in Fig. 5.

spirit of the *t*–*J* model, we choose to work in the subspace of no doubly occupied sites, but for simplicity, we do ignore the term $-\frac{J}{4} n_i n_j$ present in typical definitions of the *t*–*J* model[3]. In equation (8), we have defined a singlet creation operator on two sites as $\mathcal{S}_{ij}^\dagger = \frac{1}{\sqrt{2}}\left(c_{i\uparrow}^\dagger c_{j\downarrow}^\dagger - c_{i\downarrow}^\dagger c_{j\uparrow}^\dagger\right)$, so that H_K can be viewed as a four-site singlet-rotation term (see Fig. 1). For $K > 0$, the ground state of H_K on a single plaquette with two electrons is a d_{xy}-orbital spin-singlet; so, loosely speaking, H_K has a tendency to build *d*-wave correlations into the system and qualitatively alter the sign structure of the electronic ground state. Further arguments for studying this model in our investigation of the *d*-wave metal can be found in the Supplementary Information.

Although not particularly conventional, our ring-exchange term H_K (which should not be confused with four-site cyclic spin-exchange[38–40]) is present when projecting the continuum many-body Hamiltonian for screened Coulomb-interacting electrons into a narrow, tight-binding band[41] (see Supplementary Information). In fact, estimating the strength of K, or coefficients on related terms, in real materials such as $La_{2-x}Sr_xCuO_4$ is an interesting unresolved question.

DMRG and VMC study of two-leg model

Unfortunately, as with any interacting fermionic model, our *t*–*J*–*K* Hamiltonian suffers from the 'fermionic sign problem', rendering quantum Monte Carlo calculations inapplicable[42]. We thus follow the heretofore successful[22–24,39,40] approach of accessing 2D gapless phases by studying their quasi-1D descendants on ladder geometries, relying heavily on large-scale DMRG calculations. In fact, we have already established[22–24] that for two, three and four legs, the DBM phase itself is the stable ground state of a boson ring-exchange model analogous to equation (6). Here, we take the important first step of placing the electron ring *t*–*J*–*K* model on the two-leg ladder in search of a two-leg descendant of the *d*-wave metal.

For concreteness, we now consider the model, equation (6), on the two-leg ladder (see Fig. 1) at a generic electron density of $\rho = N_e/(2L_x) = 1/3$, where $N_e = N_{c\uparrow} + N_{c\downarrow}$ is the total number of electrons and L_x is the length of our two-leg ladder (that is, the system has $L_x \times 2$ total sites). At this density $\rho = 1/3 < 1/2$ on the two-leg ladder, the non-interacting ground state is a spin-singlet wherein electrons of each spin partially fill the bonding band ($k_y = 0$), leaving the antibonding band ($k_y = \pi$) empty. Thus, for $t \gg K$, we expect the system to be in a simple one-band metallic state, which is a two-leg analogue of the Fermi liquid. Formally speaking, this phase is a conventional Luttinger liquid with two 1D gapless modes (central charge $c = 2$). For moderate values of ring exchange, $K \gtrsim t$, we anticipate the unconventional non-Fermi-liquid *d*-wave metal to be a candidate ground state. On the two-leg ladder at this density, the *d*-wave metal phase has characteristic band-filling configurations for the d_1, d_2 and $f_{\uparrow/\downarrow}$ partons as shown in Fig. 2: d_1 partially fills both bonding and antibonding bands, whereas d_2 and $f_{\uparrow/\downarrow}$ fill only the bonding band. (The d_1 and d_2 configurations constitute the phase denoted "DBL[2,1]" in ref. 22.) In a mean-field approximation in which the partons do not interact, the system has five 1D gapless modes corresponding to the five total partially filled bands. However, in the strong-coupling limit of the full quasi-1D gauge theory (see the Supplementary Information for details), two orthonormal linear combinations of the original five modes are rendered massive, leaving an unconventional Luttinger liquid with $c = 3$ gapless modes.

We now provide extensive numerical evidence that this two-leg descendant of the *d*-wave metal exists as the ground state of the *t*–*J*–*K* model over a wide region of the phase diagram. We summarize these results in Fig. 3 by presenting the full phase diagram in the parameters K/t versus J/t as obtained by DMRG calculations on length $L_x = 24$ and 48 systems at electron density $\rho = 1/3$. For small K, we find a conventional one-band (spinful) Luttinger liquid phase which is a two-leg analogue of the Fermi-liquid metal. For moderate J and upon increasing K, the system goes into the unconventional non-Fermi-liquid *d*-wave metal phase, which is the main focus of this work. The phase boundaries in Fig. 3, all of which represent strong first-order transitions, were determined by measuring several standard momentum-space correlation functions in the DMRG (see the Supplementary Information for details): the electron momentum distribution function $\left\langle c_{qs}^\dagger c_{qs} \right\rangle$, the density–density structure factor $\left\langle \delta n_q \delta n_{-q} \right\rangle$, and the spin–spin structure factor $\left\langle \boldsymbol{S}_q \cdot \boldsymbol{S}_{-q} \right\rangle$.

For concreteness, we now focus on the cut along $J/t = 2$ in Fig. 3 for a 48×2 system with $N_e = 32$ electrons. We take one point deep within the conventional one-band metal at $K/t = 0.5$ and the other

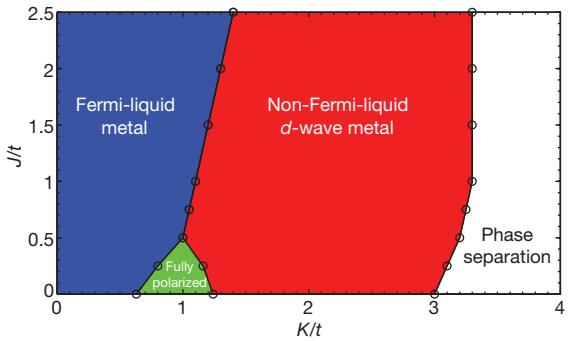

Figure 3 | Phase diagram of the *t*–*J*–*K* electron ring-exchange model at electron density $\rho = 1/3$ on the two-leg ladder. In addition to the conventional one-band metal ('Fermi-liquid metal') and exotic 'non-Fermi-liquid *d*-wave metal', there are two other realized phases. For small J, there is an intermediate phase with fully polarized electrons. For large K, owing to the inherently attractive nature of ring-exchange interactions[22], the system generally phase separates along the ladder.

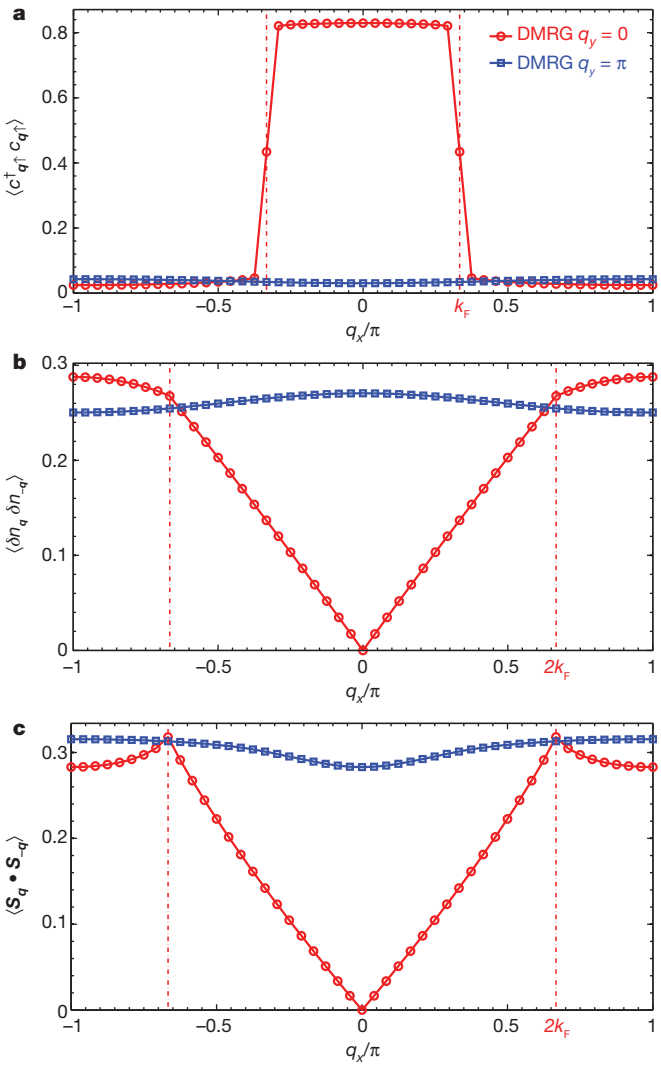

Figure 4 | DMRG measurements in the conventional Luttinger liquid phase at $J/t = 2$ and $K/t = 0.5$. We show the electron momentum distribution function (**a**), the density–density structure factor (**b**) and the spin–spin structure factor (**c**). The important wavevectors k_F and $2k_F$, as described in the text, are highlighted by vertical dashed-dotted lines.

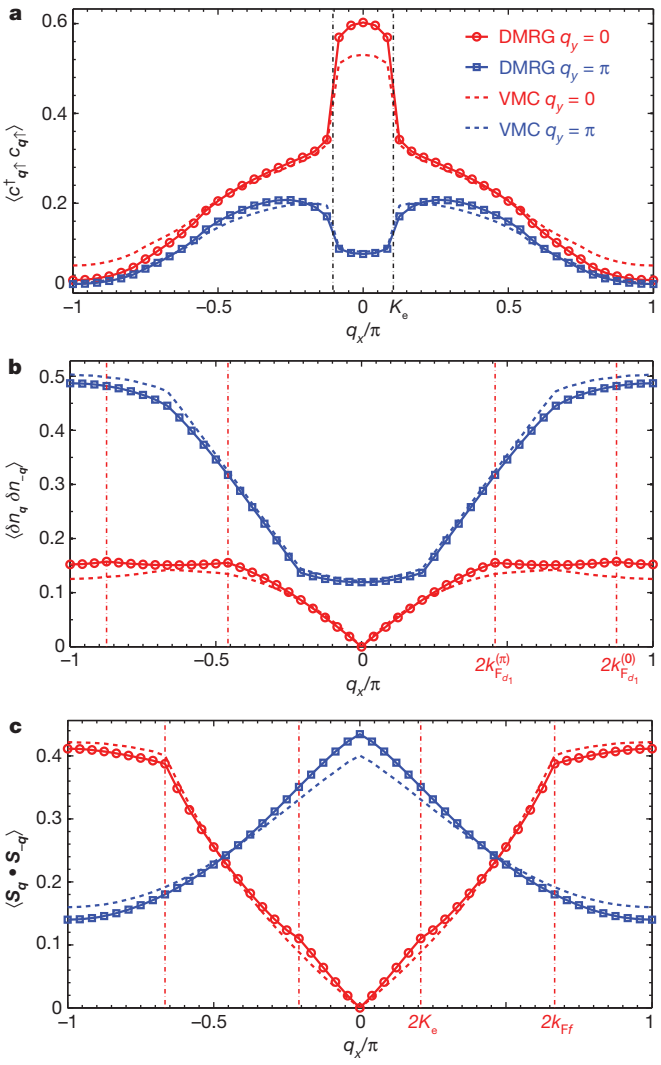

Figure 5 | DMRG measurements in the unconventional *d*-wave metal phase at $J/t = 2$ and $K/t = 1.8$. We show the same quantities as in Fig. 4. Here, we also show the matching VMC measurements using a *d*-wave metal trial wavefunction, depicted in Fig. 2.

point deep within the exotic *d*-wave metal at $K/t = 1.8$. First focusing on the former case, in Fig. 4 we show DMRG measurements characteristic of the conventional Luttinger liquid. The ground state is a spin-singlet with a sharp singularity in the electron momentum distribution function at $q_y = 0$ and $q_x = k_F = \pi N_{c\uparrow}/L_x = 8 \times 2\pi/48$, which is a usual Fermi wavevector determined solely from the electron density. The density–density and spin–spin structure factors at $q_y = 0$ also exhibit familiar features at $q_x = 0$ and $q_x = 2k_F = 16 \times 2\pi/48$, both characteristic of an ordinary one-band metallic state with gapless charge and spin modes[27]. We stress that, even with the constraint of no double-occupancy and non-zero $K/t = 0.5$ and $J/t = 2$, the interacting electronic system is still qualitatively very similar to the two-leg free Fermi gas; analogously, the 2D Fermi liquid is in many ways qualitatively similar to the 2D free Fermi gas. In both cases, the main differences are basically quantitative and are well understood[1,27].

We turn now to the characteristic point within the *d*-wave metal phase at $J/t = 2$ and $K/t = 1.8$. In Fig. 5, we show a set of DMRG measurements at this point, as well as measurements corresponding to a variational wavefunction chosen such that its singular features best reproduce the DMRG data (see the Supplementary Information for details of our VMC methods). The selected *d*-wave metal wavefunction is depicted schematically in Fig. 2. Specifically, we have the following parton Fermi wavevectors: $2k^{(0)}_{Fd_1} = 21 \times 2\pi/48$, $2k^{(\pi)}_{Fd_1} = 11 \times 2\pi/48$, $2k_{Fd_2} = 32 \times 2\pi/48$, and $2k_{Ff} = 16 \times 2\pi/48$. The overall agreement between the DMRG and VMC measurements is very compelling, and we now summarize our understanding of these results from the perspective of *d*-wave metal theory.

In sharp contrast to the conventional Luttinger liquid, the electron momentum distribution function now has singularities for both $q_y = 0$ and $q_y = \pi$ at a wavevector $q_x = K_e \equiv [k^{(0)}_{Fd_1} - k^{(\pi)}_{Fd_1}]/2$. This wavevector corresponds to a composite electron made from a combination of parton fields consisting of a right-moving d_1 parton, a left-moving d_2 parton, and a right-moving spinon: $d^{(q_y)}_{1R} d_{2L} f_{\uparrow R}$. In fact, these 'enhanced electrons' can be guessed from simple 'Amperian rules'[3,43,44] in our quasi-1D gauge theory, as described in detail in the Supplementary Information.

The corresponding density–density and spin–spin structure factors, displayed in Fig. 5b and c, also show nontrivial behaviour. We expect the density–density structure factor to be sensitive to each parton configuration individually and thus have singular features at various '$2k_F$' parton wavevectors (see refs 21, 23 and the Supplementary Information). In the DMRG measurements, the most noticeable features are at $q_y = 0$ and $q_x = 2k^{(0)}_{Fd_1}$, $2k^{(\pi)}_{Fd_1}$, which allow

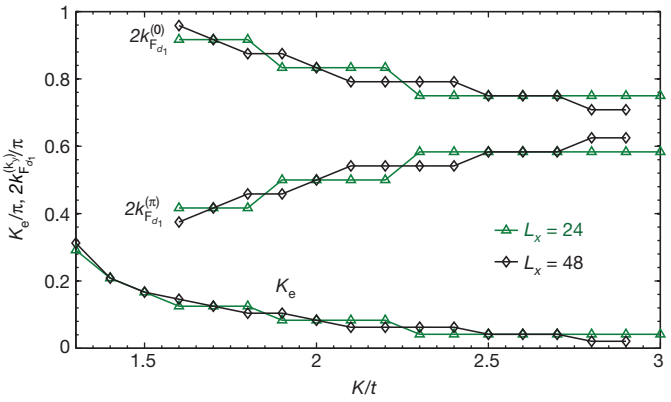

Figure 6 | Evolution of singular wavevectors in the *d*-wave metal phase. At fixed $J/t = 2$ and varying K/t, we show the location of the dominant singular wavevector K_e in the electron momentum distribution function (see Fig. 5a), as well as the wavevectors identified as $2k^{(0)}_{Fd_1}$ and $2k^{(\pi)}_{Fd_1}$ in the density–density structure factor (see Fig. 5b). These calculations were done with DMRG.

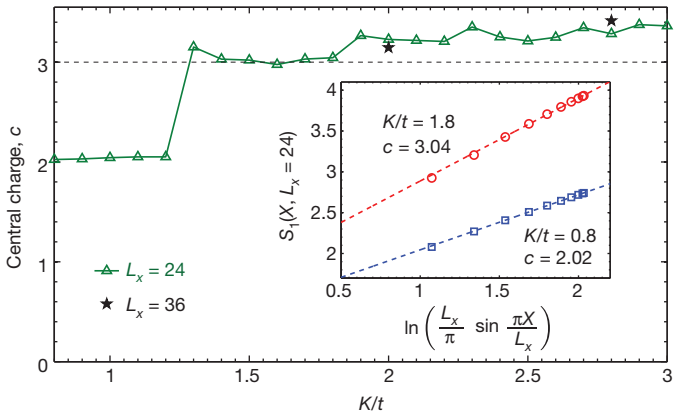

Figure 7 | Central charge *c* as a function of interaction *K*/*t*. By measuring the von Neumann entanglement entropy S_1 in the DMRG, we calculate the effective central charge c at fixed $J/t = 2$ and varying K/t. There is a dramatic jump from $c \simeq 2$ to $c \simeq 3$ at the transition, as predicted by our theory. Data for two example points—$K/t = 0.8$ and 1.8—are shown in the inset, where X is the number of rungs in each bipartition. (See also the Supplementary Information.)

us to read off directly the realized d_1 parton configuration (see Fig. 2). The lack of these features in the VMC data, as well as the lack of analogous features at $q_x = 2k_{Fd_2}$ in the DMRG data, can be understood within our gauge theory framework as presented in the Supplementary Information, where we also note that our wavefunction is only a caricature of the full theory. Finally, the spin–spin structure factor at $q_y = 0$ not only has a familiar, expected feature at $q_x = 2k_{Ff}$ coming from the spinon, but also remarkably contains a feature at $q_x = 2K_e$ that can be thought of as a '$2k_F$' wavevector from the dominant 'electron' in Fig. 5a. All in all, as we further explain in the Supplementary Information, the DMRG measurements are consistent, even on a fine quantitative level, with being in a stable non-Fermi-liquid *d*-wave metal phase.

We note that the wavevector K_e depends on the interaction strength K/t because the wavevectors $k^{(0)}_{Fd_1}$ and $k^{(\pi)}_{Fd_1}$ vary with ring exchange[22]. In Fig. 6, we show at $J/t = 2$ evolution with K/t of the wavevector K_e, that is, the location of the sharp steps in the electron momentum distribution function (see Fig. 5a), as determined by DMRG. Given that the momentum-space 'volume' enclosed by these singular features depends on the interaction K/t and is not simply determined by the total density of electrons, we may confidently say that the *d*-wave metal violates Luttinger's volume theorem[7]. In fact, the very notion of a single 'Fermi surface' is actually ambiguous in the *d*-wave metal phase. We also show in Fig. 6, for those values of K/t at which they are discernible, the wavevectors $2k^{(0)}_{Fd_1}$ and $2k^{(\pi)}_{Fd_1}$ as identified by features in the DMRG-measured density–density structure factor at $q_y = 0$ (see Fig. 5b). For all points, the locations of the identified features satisfy the nontrivial identity $K_e = [2k^{(0)}_{Fd_1} - 2k^{(\pi)}_{Fd_1}]/4$, as predicted by our theory.

A remarkable property of the *d*-wave metal state found in the DMRG is that it has prominent critical *d*-wave Cooper pairs residing on the diagonals, as anticipated earlier from the ring energetics (see the Supplementary Information). Such Cooper pair correlations have the slowest power-law decay of all the discussed observables, including the electron Green's function. This is in stark contrast with a conventional metal and suggests that the *d*-wave metal phase has some incipient *d*-wave superconductivity in two dimensions.

As a final piece of evidence that the realized DMRG phase is in fact the *d*-wave metal, we have measured the number of 1D gapless modes, that is, the effective central charge c, via scaling of the bipartite entanglement entropy[45,46] in the DMRG and VMC[47,48] wavefunctions. As explained above, we expect $c = 2$ in the conventional Luttinger liquid and $c = 3$ in the *d*-wave metal. See the Supplementary Information for a detailed comparison of the DMRG and VMC entropy measurements, where we show that the DMRG–VMC agreement is just as impressive as it is for the more traditional measurements of Fig. 5. The effective central charge versus K/t at $J/t = 2$ as determined by the DMRG is shown in Fig. 7. Indeed, these measurements indicate that $c \simeq 2$ in the conventional one-band metal, whereas $c \simeq 3$ in the exotic *d*-wave metal. Because $c = 3 > 2$, our putative *d*-wave metal phase clearly cannot be understood as an instability out of the conventional one-band metal, but also, because $c = 3 < 4$, the critical bonding and antibonding electrons in Fig. 5a cannot be reproduced by any perturbative treatment starting from free electrons[31] (see also the Supplementary Information).

Discussion and outlook

Here we have presented strong evidence for the stability of a two-leg descendant of our exotic strange-metal phase, the *d*-wave metal, and we conclude with an outlook on exciting future work. Firstly, our present two-leg *d*-wave metal treatment is readily extendable to systems with more legs. Ref. 24 established the stability of the *d*-wave Bose metal, the main ingredient of the *d*-wave metal, on three- and four-leg ladders. Thus, we do not envision any conceptual obstacles in the way of realizing a similar result for the *d*-wave metal. However, we do anticipate that adding more legs will be very challenging numerically for the DMRG owing to the large amount of spatial entanglement present in the *d*-wave metal and Fermi liquid—this is also the current limitation preventing modern 2D tensor network state methods from attacking such problems[49].

With the goal of connecting to experiments, it would be desirable to perform a detailed energetics study of the *t*–*J*–*K* model in two dimensions and explore the applicability of such models to strongly correlated materials. By studying 2D variational wavefunctions based on the *d*-wave metal, it should be possible to compare physical properties with experimentally observed strange metals, such as that in the copper oxides. This could include various instabilities of the *d*-wave metal, such as spinon pairing as a model of a pseudogap metal or chargon pairing as a model of an "orthogonal metal", discussed recently[50]. The *d*-wave sign structure already inherent in the non-superconducting parent *d*-wave metal suggests that there may be incipient *d*-wave superconductivity of the copper-oxide variety, which is particularly exciting. Although we have stressed its Luttinger volume violation as a characteristic non-Fermi liquid property of the *d*-wave metal, we note that the 2D phase will also have no Landau quasiparticle as well as exhibit non-Fermi-liquid-like thermodynamics and transport. Comparing these predictions with properties of real strange metals would be interesting. In the end, however, we stress the conceptual nature of the present study, and hope that our ideas may open up new avenues for thinking about non-Fermi liquid electronic fluids.

Received 1 August; accepted 29 October 2012.
Published online 19 December 2012.

1. Baym, G. & Pethick, C. *Landau Fermi-Liquid Theory: Concepts and Applications* (Wiley-VCH, Germany, 1991).
2. Schofield, A. J. Non-Fermi liquids. *Contemp. Phys.* **40,** 95–115 (1999).
3. Lee, P. A., Nagaosa, N. & Wen, X.-G. Doping a Mott insulator: physics of high-temperature superconductivity. *Rev. Mod. Phys.* **78,** 17–85 (2006).
4. Boebinger, G. S. An abnormal normal state. *Science* **323,** 590–591 (2009).
5. Stewart, G. R. Non-Fermi-liquid behavior in *d*- and *f*-electron metals. *Rev. Mod. Phys.* **73,** 797–855 (2001).
6. Gegenwart, P., Si, Q. & Steglich, F. Quantum criticality in heavy-fermion metals. *Nature Phys.* **4,** 186–197 (2008).
7. Luttinger, J. M. Fermi surface and some simple equilibrium properties of a system of interacting fermions. *Phys. Rev.* **119,** 1153–1163 (1960).
8. Anderson, P. W. & Zou, Z. "Normal" tunneling and "normal" transport: diagnostics for the resonating-valence-bond state. *Phys. Rev. Lett.* **60,** 132–135 (1988).
9. Varma, C. M., Littlewood, P. B., Schmitt-Rink, S., Abrahams, E. & Ruckenstein, A. E. Phenomenology of the normal state of Cu-O high-temperature superconductors. *Phys. Rev. Lett.* **63,** 1996–1999 (1989).
10. Senthil, T. Critical Fermi surfaces and non-Fermi liquid metals. *Phys. Rev. B* **78,** 035103 (2008).
11. Faulkner, T., Iqbal, N., Liu, H., McGreevy, J. & Vegh, D. Strange metal transport realized by gauge/gravity duality. *Science* **329,** 1043–1047 (2010).
12. Sachdev, S. Holographic metals and the fractionalized Fermi liquid. *Phys. Rev. Lett.* **105,** 151602 (2010).
13. Anderson, P. W. The resonating valence bond state in La_2CuO_4 and superconductivity. *Science* **235,** 1196–1198 (1987).
14. Baskaran, G., Zou, Z. & Anderson, P. W. The resonating valence bond state and high-Tc superconductivity – a mean field theory. *Solid State Commun.* **63,** 973–976 (1987).
15. Nagaosa, N. & Lee, P. A. Normal-state properties of the uniform resonating-valence-bond state. *Phys. Rev. Lett.* **64,** 2450–2453 (1990).
16. Lee, P. A. & Nagaosa, N. Gauge theory of the normal state of high-T_c superconductors. *Phys. Rev. B* **46,** 5621–5639 (1992).
17. Wen, X.-G. & Lee, P. A. Theory of underdoped cuprates. *Phys. Rev. Lett.* **76,** 503–506 (1996).
18. Anderson, P. W., Baskaran, G., Zou, Z. & Hsu, T. Resonating valence-bond theory of phase transitions and superconductivity in La_2CuO_4-based compounds. *Phys. Rev. Lett.* **58,** 2790–2793 (1987).
19. Feigelman, M. V., Geshkenbein, V. B., Ioffe, L. B. & Larkin, A. I. Two-dimensional Bose liquid with strong gauge-field interaction. *Phys. Rev. B* **48,** 16641–16661 (1993).
20. Cooper, R. A. *et al.* Anomalous criticality in the electrical resistivity of $La_{2-x}Sr_xCuO_4$. *Science* **323,** 603–607 (2009).
21. Motrunich, O. I. & Fisher, M. P. A. *d*-wave correlated critical Bose liquids in two dimensions. *Phys. Rev. B* **75,** 235116 (2007).
22. Sheng, D. N., Motrunich, O. I., Trebst, S., Gull, E. & Fisher, M. P. A. Strong-coupling phases of frustrated bosons on a two-leg ladder with ring exchange. *Phys. Rev. B* **78,** 054520 (2008).
23. Block, M. S. *et al.* Exotic gapless Mott insulators of bosons on multileg ladders. *Phys. Rev. Lett.* **106,** 046402 (2011).
24. Mishmash, R. V. *et al.* Bose metals and insulators on multileg ladders with ring exchange. *Phys. Rev. B* **84,** 245127 (2011).
25. White, S. R. Density matrix formulation for quantum renormalization groups. *Phys. Rev. Lett.* **69,** 2863–2866 (1992).
26. White, S. R. Density-matrix algorithms for quantum renormalization groups. *Phys. Rev. B* **48,** 10345–10356 (1993).
27. Giamarchi, T. *Quantum Physics in One Dimension* (Oxford Univ. Press, 2003).
28. Shankar, R. Bosonization: how to make it work for you in condensed matter. *Acta Phys. Polon. B* **26,** 1835–1867 (1995).
29. Lin, H.-H., Balents, L. & Fisher, M. P. A. Exact SO(8) symmetry in the weakly-interacting two-leg ladder. *Phys. Rev. B* **58,** 1794–1825 (1998).
30. Fjærestad, J. O. & Marston, J. B. Staggered orbital currents in the half-filled two-leg ladder. *Phys. Rev. B* **65,** 125106 (2002).
31. Balents, L. & Fisher, M. P. A. Weak-coupling phase diagram of the two-chain hubbard model. *Phys. Rev. B* **53,** 12133–12141 (1996).
32. Ceperley, D., Chester, G. V. & Kalos, M. H. Monte Carlo simulation of a many-fermion study. *Phys. Rev. B* **16,** 3081–3099 (1977).
33. Gros, C. Physics of projected wavefunctions. *Ann. Phys.* **189,** 53–88 (1989).
34. Hellberg, C. S. & Mele, E. J. Phase diagram of the one-dimensional *t-J* model from variational theory. *Phys. Rev. Lett.* **67,** 2080–2083 (1991).
35. Ceperley, D. M. Fermion nodes. *J. Stat. Phys.* **63,** 1237–1267 (1991).
36. Halperin, B. I., Lee, P. A. & Read, N. Theory of the half-filled Landau level. *Phys. Rev. B* **47,** 7312–7343 (1993).
37. Laughlin, R. B. Anomalous quantum Hall effect: an incompressible quantum fluid with fractionally charged excitations. *Phys. Rev. Lett.* **50,** 1395–1398 (1983).
38. Normand, B. & Oleś, A. M. Circulating-current states and ring-exchange interactions in cuprates. *Phys. Rev. B* **70,** 134407 (2004).
39. Sheng, D. N., Motrunich, O. I. & Fisher, M. P. A. Spin Bose-metal phase in a spin-1/2 model with ring exchange on a two-leg triangular strip. *Phys. Rev. B* **79,** 205112 (2009).
40. Block, M. S., Sheng, D. N., Motrunich, O. I. & Fisher, M. P. A. Spin Bose-metal and valence bond solid phases in a spin-1/2 model with ring exchanges on a four-leg triangular ladder. *Phys. Rev. Lett.* **106,** 157202 (2011).
41. Imada, M. & Miyake, T. Electronic structure calculation by first principles for strongly correlated electron systems. *J. Phys. Soc. Jpn* **79,** 112001 (2010).
42. Troyer, M. & Wiese, U.-J. Computational complexity and fundamental limitations to fermionic quantum Monte Carlo simulations. *Phys. Rev. Lett.* **94,** 170201 (2005).
43. Polchinski, J. Low-energy dynamics of the spinon-gauge system. *Nucl. Phys. B* **422,** 617–633 (1994).
44. Altshuler, B. L., Ioffe, L. B. & Millis, A. J. Low-energy properties of fermions with singular interactions. *Phys. Rev. B* **50,** 14048–14064 (1994).
45. Calabrese, P. & Cardy, J. Entanglement entropy and quantum field theory. *J. Stat. Mech.* **2004,** P06002 (2004).
46. Calabrese, P., Campostrini, M., Essler, F. & Nienhuis, B. Parity effects in the scaling of block entanglement in gapless spin chains. *Phys. Rev. Lett.* **104,** 095701 (2010).
47. Hastings, M. B., González, I., Kallin, A. B. & Melko, R. G. Measuring Renyi entanglement entropy in quantum Monte Carlo simulations. *Phys. Rev. Lett.* **104,** 157201 (2010).
48. Zhang, Y., Grover, T. & Vishwanath, A. Entanglement entropy of critical spin liquids. *Phys. Rev. Lett.* **107,** 067202 (2011).
49. Corboz, P., Orús, R., Bauer, B. & Vidal, G. Simulation of strongly correlated fermions in two spatial dimensions with fermionic projected entangled-pair states. *Phys. Rev. B* **81,** 165104 (2010).
50. Nandkishore, R., Metlitski, M. A. & Senthil, T. Orthogonal metals: the simplest non-Fermi liquids. *Phys. Rev. B* **86,** 045128 (2012).

Supplementary Information is available in the online version of the paper.

Acknowledgements We thank T. Senthil, R. Kaul, L. Balents, S. Sachdev, A. Vishwanath and P. Lee for discussions. This work was supported by the NSF under the KITP grant PHY05-51164 and the MRSEC programme under award number DMR-1121053 (H.-C.J.), the NSF under grants DMR-1101912 (M.S.B., R.V.M., J.R.G. and M.P.A.F.), DMR-1056536 (M.S.B.), DMR-0906816 and DMR-1205734 (D.N.S.), DMR-0907145 (O.I.M.), and by the Caltech Institute of Quantum Information and Matter, an NSF Physics Frontiers Center with the support of the Gordon and Betty Moore Foundation (O.I.M. and M.P.A.F.). We also acknowledge support from the Center for Scientific Computing from the CNSI, MRL: an NSF MRSEC award (DMR-1121053), and an NSF grant (CNS-0960316).

Author Contributions All authors made significant contributions to the research underlying this paper.

Author Information Reprints and permissions information is available at www.nature.com/reprints. The authors declare no competing financial interests. Readers are welcome to comment on the online version of the paper. Correspondence and requests for materials should be addressed to R.V.M. (mishmash@physics.ucsb.edu).